

Direct Measurement of Pressure-Independent Aqueous Humour Flow using *iPerfusion*

Michael Madekurozwa, Ester Reina-Torres, Darryl R. Overby, Joseph M. Sherwood

Syringe Pump Characterisation

In the present study, we used a syringe pump in conjunction with *iPerfusion*. It is therefore necessary to characterise the syringe pump output and its influence on the eye. In this supplementary information, we measure the raw output from the syringe pump and analyse the steady and oscillatory components of the output flow rate. We then analyse the system using a lumped parameter model to ascertain whether oscillations in the output flow rate are expected to translate to physiologically relevant changes in pressure or flow within the eye.

S-1 Syringe Pump Output

Fig. S-1a shows a tracing of the flow rate delivered by the syringe pump setup used in this study (Harvard PhD Ultra, 50 μl Hamilton gastight syringe), as measured by directly attaching the flow sensor (Sensirion SLG64) to the syringe. The pump was set to deliver 120 nl/min . The measured flow rate was $119.9 \pm 34.0 \text{ nl}/\text{min}$ (mean \pm 2SD), indicating excellent accuracy, but with large variability. This variability arises from the mechanics of the syringe pump itself. A fast Fourier transform (FFT) of the signal (Fig. S-1b) reveals a complex waveform with multiple frequencies, the causes of which can be identified based on the system mechanics.

The Harvard PhD Ultra syringe pump is driven by a stepper motor (400 steps per revolution, 1/16th microstepping), coupled to a lead screw (2mm pitch) by a belt drive with a 2:1 gear ratio (20 and 10 teeth respectively). At 120 nl/min , for a syringe with an internal diameter of 1.031 mm, the plunger velocity is 2.4 $\mu\text{m}/\text{s}$.

The lead screw rotation frequency can be calculated according to the ratio of the plunger velocity to the lead screw pitch, and is given by $f_{\text{lead screw}} = 0.0012 \text{ Hz}$. For each rotation of the lead screw, the stepper motor completes two full revolutions, hence $f_{\text{motor}} = 0.0024 \text{ Hz}$. A clear peak in the FFT can be observed at f_{motor} in Fig. S-1b. The signal component at this frequency has an amplitude of $\sim 2.5 \text{ nl}/\text{min}$ and is visualised in red on Fig. S-1a.

The next strongest peak is at $f_{\text{teeth}} = 0.0479 \text{ Hz}$, which corresponds to $20f_{\text{motor}}$, implying that the teeth on the belt drive impart this frequency response, indicated in Fig. S-1c. However, the amplitude of both these oscillation frequencies is relatively low and the main source of noise arises from the stepper motor step size.

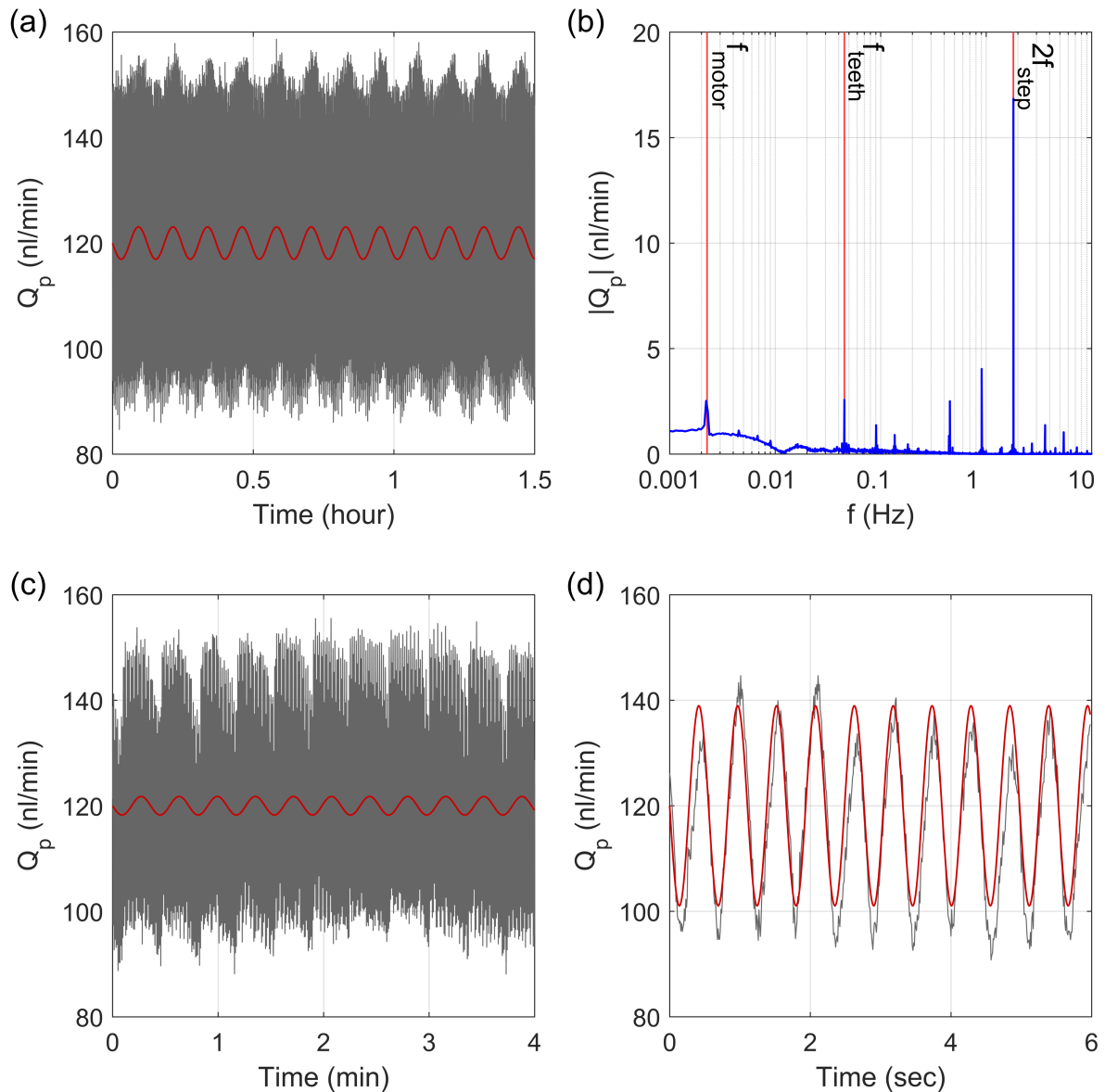


Figure S-1: Characterisation of the syringe pump output, measured directly using the flow sensor. (a,c,d) Raw signals are indicated in grey, with specific oscillation modes indicated in red. The three dominant frequencies are indicated on time scales of (a) hours - f_{motor} , (c) minutes - f_{teeth} and (d) seconds - $2f_{\text{step}}$. (b) Frequency spectrum of the pump flow rate oscillations.

The stepping frequency of the stepper motor can be calculated as the number of steps per revolution times the motor frequency, giving $f_{\text{step}} = 0.958 \text{ Hz}$, which can be seen as a peak at $\sim 4 \text{ nl/min}$ in Fig. S-1b, with a subharmonic at $0.5f_{\text{step}}$. The strongest peak occurs at $2f_{\text{step}}$ with an amplitude of $\sim 17 \text{ nl/min}$, and the oscillations observed at this frequency can be clearly observed in Fig. S-1d. This peak, at twice the stepping frequency, corresponds to the frequency of polarity reversal within the stepper motor coils.

Note that, as the mechanical components are all coupled, the oscillations at different frequencies are all in phase, and hence their amplitudes contribute to the 2SD level of $\pm 34 \text{ nl/min}$ (which would not necessarily be the case if some components were out of phase).

S-2 Damping Effects

The oscillations output by the syringe pump will not be equal to those experienced by the eye, due to the compliances and resistances in the system:

- Ocular compliance - ϕ_e
- Tubing compliances - ϕ_t (tubes connecting to both *iPerfusion* and the syringe pump)
- Needle resistances - R_n (each needle)
- Flow sensor resistance - R_q
- Eye resistance - R_e (reciprocal of the facility)

For analysing the damping effect on oscillations, we consider the impedances, Z , of key system components. Fig. S-2a shows a lumped parameter model of the entire system and eye, using impedance elements.

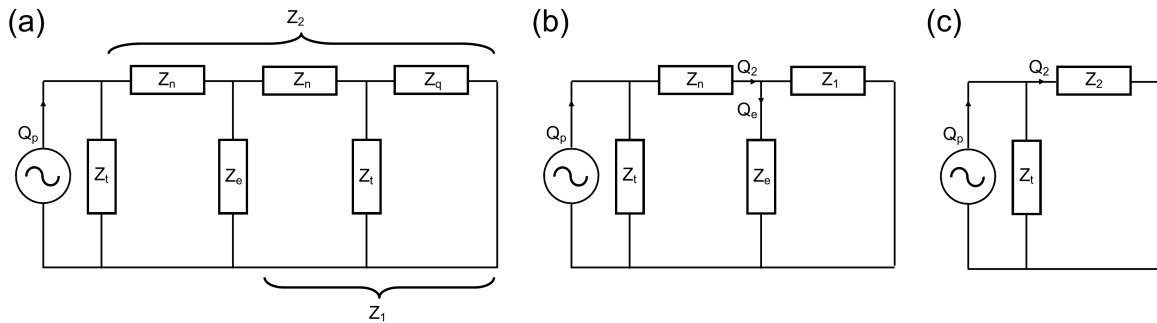


Figure S-2: Lumped parameter models showing the key impedances of the system and eye. Q_p is the oscillatory response of the syringe pump, Z_t is the impedance of the connecting tubes, Z_e is the impedance of the eye, Z_q is the impedance of the flow sensor and Z_n is the impedance of the needles. (a) Complete system, (b) after reducing the *iPerfusion* system to a single impedance (Z_1), (c) after a further reduction yielding an impedance Z_2 , comprising the *iPerfusion* system, the eye, and the needle connected to the syringe pump.

The impedance of the eye, comprising ϕ_e and R_e in parallel (\parallel), is given by

$$Z_e = R_e \parallel \phi_e = \frac{R_e}{2j\pi f \phi_e R_e + 1} \quad (\text{S-1})$$

where j is the unit imaginary number and f is the oscillation frequency. The impedance of the tubing (60 cm blood perfusion tubing) is given by

$$Z_t = \frac{1}{2j\pi f \phi_t} \quad (\text{S-2})$$

For resistive elements, the impedance is equal to the resistance, hence $Z_q = R_q$ and $Z_n = R_n$. In order to analyse the circuit, we first combine the impedances of the flow sensor, and the tubing and needle connecting the eye to the *iPerfusion* system, Z_1 , as shown in Fig. S-2b.

$$Z_1 = Z_q || Z_t + Z_n \quad (\text{S-3})$$

We subsequently combine this resistance with the impedances of the eye and the needle connecting the eye to the syringe pump, as shown in Fig. S-2c, to give

$$Z_2 = Z_e || Z_1 + Z_n \quad (\text{S-4})$$

We can now calculate the proportion of oscillatory flow entering the combined impedance Z_2 according to

$$Q_2 = Q_p \left(\frac{Z_t}{Z_2 + Z_t} \right) \quad (\text{S-5})$$

Then using Fig. S-2b, the amount of flow entering the eye is

$$Q_e = Q_2 \left(\frac{Z_1}{Z_1 + Z_e} \right) \quad (\text{S-6})$$

For a given frequency, the gain is defined as the amplitude of the flow into the eye, relative to that output by the pump:

$$\text{Gain} = \left| \frac{Q_e}{Q_p} \right| = \left| \frac{Z_1 Z_t}{(Z_1 + Z_e)(Z_2 + Z_t)} \right| \quad (\text{S-7})$$

Equation S-7 can be used to estimate the flow oscillations in the eye using the syringe pump output (Fig. S-1b) and typical parameters for the system and mouse eye, listed in Table S-1.

Table S-1: Typical parameters for a mouse eye at 8 mmHg

Parameter	Value	Unit
R_e	0.16	mmHg/(nl/min)
R_q	0.01	mmHg/(nl/min)
R_n	0.0002	mmHg/(nl/min)
ϕ_t	15	nl/mmHg
ϕ_e	50	nl/mmHg

Fig. S-3a shows that the frequency response of the flow into the eye is damped as compared to the pump output (Fig S-1b). The major oscillations at $2f_{\text{step}}$ are reduced to $\sim 7 \text{ nl/min}$, and the low frequency components are also reduced. Using an inverse FFT, we can estimate the flow rate into the compliance of the eye (blue trace in Fig. S-3b). The 2SD value for this signal is $\pm 7.5 \text{ nl/min}$, and is hence reduced almost five-fold relative to the syringe pump output. It is interesting to note

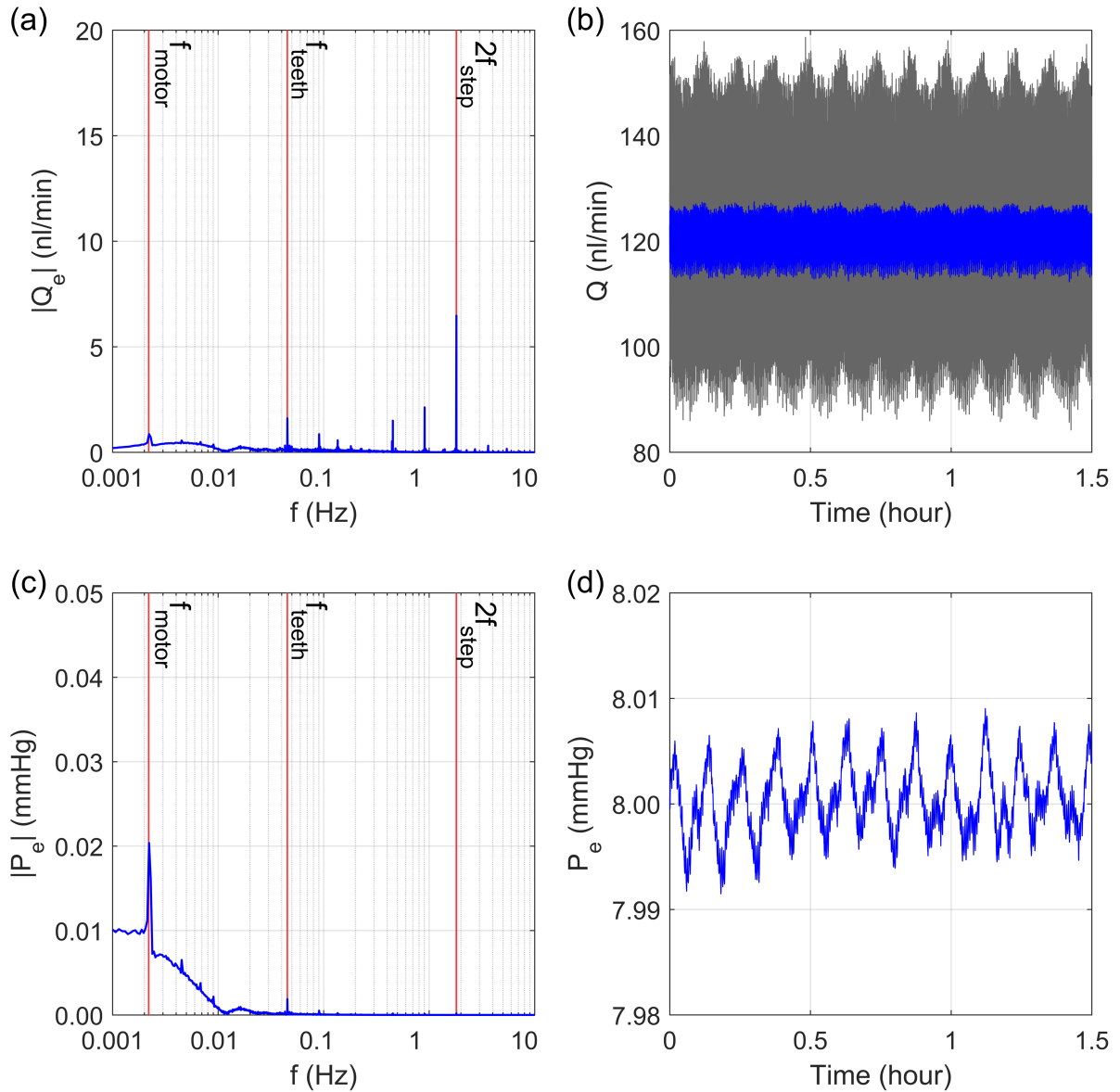


Figure S-3: Effect of damping on the the oscillations entering the eye from the syringe pump. (a) Predicted frequency spectra of the oscillations in flow rate entering the compliance of the eye, (b) predicted flow trace in the eye using inverse FFT (blue), compared to pump output (grey), (c) predicted frequency spectra of the oscillations in intraocular pressure, (d) predicted pressure trace in the eye using inverse FFT.

that, as the phases of some of the frequency components would be altered, the combined amplitude is similar to the main peak at $2f_{\text{step}}$.

Finally, we consider the effect that this oscillatory flow has on the pressure in the eye. We first calculate the FFT for the intraocular pressure, as shown in Fig. S-3c, according to

$$P_e = Q_e Z_e \quad (\text{S-8})$$

The low frequencies are maintained, but frequencies above 0.01 Hz are almost entirely damped. Fig. S-3d shows the predicted pressure tracing based on the inverse FFT, around a mean pressure of 8 mmHg . Here, the frequency of the motor has the largest effect on intraocular pressure variations, with a peak to peak oscillation amplitude of $\sim 0.015 \text{ mmHg}$, but with a period of $\sim 7 \text{ min}$.

In summary, the syringe pump output is highly oscillatory, but in our system the oscillations are largely damped, such that the intraocular pressure variation is unlikely to have an effect on the physiology of the aqueous humour dynamics investigated in this study.